Journal of Life Sciences & Biomedicine, vol. 6(79), No 2, p. 13-32 (2024)

Does molecular docking between the cement protein of barnacles and resin acids open a new gate for the development of eco-friendly antifouling paint?

Ibrahim Kirkiz, Levent Cavas*

Department of Chemistry (Biochemistry Division), Faculty of Science, Dokuz Eylül University, Kaynaklar Campus, 35390, İzmir, Türkiye

***For correspondence:** levent.cavas@deu.edu.tr*

Received: September 1, 2024; Received in revised form: October 17, 2024; Accepted: November 6, 2024

As a result of the surfaces of ships being covered with fouling organisms, ships begin to consume more fuel to reach their destinations. Excessive fuel consumption by ships causes carbon emissions to increase. This increase in carbon emissions is one of the main reasons for climate change and biodiversity loss because it causes ocean acidification. Another factor affecting biodiversity is antifouling paints containing biocides. In antifouling paints, released compounds accumulate in sediments and marine organisms. These compounds interact differently with various organisms to achieve antifouling abilities. To understand the molecular interactions between cement proteins from *Amphibalanus amphitrite* and resin acids, molecular docking was carried out comprehensively in the present study. For molecular docking, CB-Docking was used to estimate the bonding energies. According to the results, the best interaction was found between dehydroabietic acid and *A. amphitrite* CP-20k-2 and the binding energy was -8.0 kcal/mol. The weakest binding energy was observed between neoabietic acid and *A. amphitrite* CP-20k-1 with -4.7 kcal/mol. In conclusion, the molecular docking between specific proteins responsible for fouling activity and the chemical that will be used in the formulation of new eco-friendly antifouling paints can correctly estimate the antifouling performance. Moreover, the *in-silico* methods can decrease the cost and time for R&D studies of new-generation eco-friendly antifouling paints.

***Keywords:** Biofouling, antifouling, barnacles, cement protein, molecular docking*

INTRODUCTION

Marine biofouling is the attachment of living organisms to surfaces that are immersed in marine environments (Gule et al., 2016). Both organic and inorganic materials can attach to the surfaces, making total accumulation on the surface easier. Fouling organisms, such as barnacles, tubeworms, and mussels, adhere to surfaces and populate. This phenomenon can occur on any surface immersed in seawater. In general terms, biofouling occurs in several steps. The first step is the enrichment of the surface with organic materials, which is called the conditioning film layer. This process takes minutes to form. The formation and contents of the conditioning film layer are crucial for the attachment of marine organisms. Subsequently, microorganisms start populating the film layer, and as time passes, more organisms attach to the surface, including macrofouling organisms such as barnacles and mussels (Yebra et al., 2004; Sarkar et al., 2022).

Biofouling has some negative effects on marine-related industries. Biofouling can cause clogging in pipes, filter systems, and aquaculture nets. However, the main reason that marine biofouling draws much attention is its effects on marine vessels. In particular, the hulls and propellers of ships are negatively affected by biofouling. Normally, hulls are smooth surfaces, but with biofouling, the surface becomes rough, thus increasing surface friction. Increased surface friction will decrease the speed, and this will cause the consumption of more fuel to

https://doi.org/10.59849/2710-4915.2024.2.13
Available online 31 December 2024

compensate for the speed loss. Biofouling can also cause the transportation of invasive species to different ecosystems. This issue negatively affects the biodiversity of ecosystems because most invasive species are aggressive toward other organisms (Carve et al., 2019; Farkas et al., 2021).

There are different types of fouling organisms, but barnacles are the most studied species. The reason for this is their adhesion mechanisms. Barnacles use an adhesive called cement to attach surfaces underwater (Kamino, 2013; Liang et al., 2019; Dreyer et al., 2020). Because of this feature, scientists are studying barnacle cement to create commercial adhesives that perform in the same way underwater.

Barnacles are sessile crustaceans. Because they do not have any limbs to move themselves, they move around by the movements of the water column (Kamino et al., 2012; Ip et al., 2021). Barnacles go through four phases in their lives. Nauplius is the larval stage of a barnacle (Nasrolahi et al., 2016; Ewers-Saucedo and Pappalardo, 2019). Nauplius transforms into cyprids when they grow to a sufficient size (Kamino, 2016; Liu et al., 2016). Cyprids move around with the movements of the water column to seek a surface to settle. Their primary function is to find a surface to settle (Aldred and Clare, 2008). When cyprids find a suitable surface, they secrete a temporary adhesive called a footprint (Yap et al., 2017). With this adhesive, cyprids attach to surfaces reversibly. After this stage, the cyprid transforms into a juvenile barnacle. Then, the juvenile becomes an adult barnacle and secretes cement to irreversibly attach. Cement is secreted from the cement gland (Kamino, 2016; Yan et al., 2020).

Cement contains approximately 85% protein, but not all of them have been identified (Walker, 1972; Kamino et al., 1996). Different cement proteins are used in underwater adhesion, and they all have different functions. On the other hand, there are some proteins that have been identified according to their functions. CP-100k and CP-52k are hydrophobic proteins with high molecular weights. They are the main components of cement that hold other molecules together (Kamino, 2016; Rocha et al., 2019; Wong et al., 2023). CP-68k contains charged amino acids. Therefore, it might be responsible for interactions with foreign surfaces (Yuvaraj et al., 2021). There are also small polypeptides such as CP-20k. CP-20k does not bond with other cement proteins, and because of this feature, it is likely a coupling agent that interacts with another barnacle cement (Jonker et al., 2014; Li et al., 2021). CP-19k contains amino acid compounds similar to CP-68k. CP-19k is absorbed by different materials such as glass and polystyrene. Therefore, CP-19k may be responsible for the adhesion process (Rocha et al., 2019). Another small protein is CP-16k, which has similarities with litotic enzymes. With this feature, CP-16k protects the cement structure from marine micro and macro organisms (Li et al., 2021).

With the regulations brought to the antifouling technology, more and more compounds are being tested for their natural antifouling abilities (Almeida and Vasconcelos, 2015). Methods used to determine the performance of antifouling paints require time, labor, and money. When the chosen natural compound does not perform as desired in seawater, the above resources are wasted. For this reason, *in silico* tools can be used to at least have an idea about the interactions between natural compounds and target molecules (Assadizadeh et al., 2023; Cavas and Dağ, 2024).

The search for natural bioactive materials is increasing rapidly. Resin is one of those materials because trees release it to deal with infections due to pathogens. In particular, resin acids have great potential because of their antimicrobial activities (Savluchinske-Feio et al., 2006; Dimkić et al., 2016). Resin acids have functional groups such as aldehydes, hydroxyls, and ketones to increase their antimicrobial performance. Resin acids mostly consist of terpenoids. Rosin, a rich source of diterpenes, is obtained from pine resin after steam distillation (Ottavioli et al., 2019). Diterpene resin acids are 20-carbon and cyclic carboxylic acids. Rosin contains tricyclic diterpene acids such as abietic, dehydroabietic, isopimaric, levopimaric, neoabietic, palustric, pimaric, and sandaracopimaric acids (Martin et al., 1999; Keeling and Bohlmann, 2006). The tricyclic structures of diterpenes are given in Figure 1.

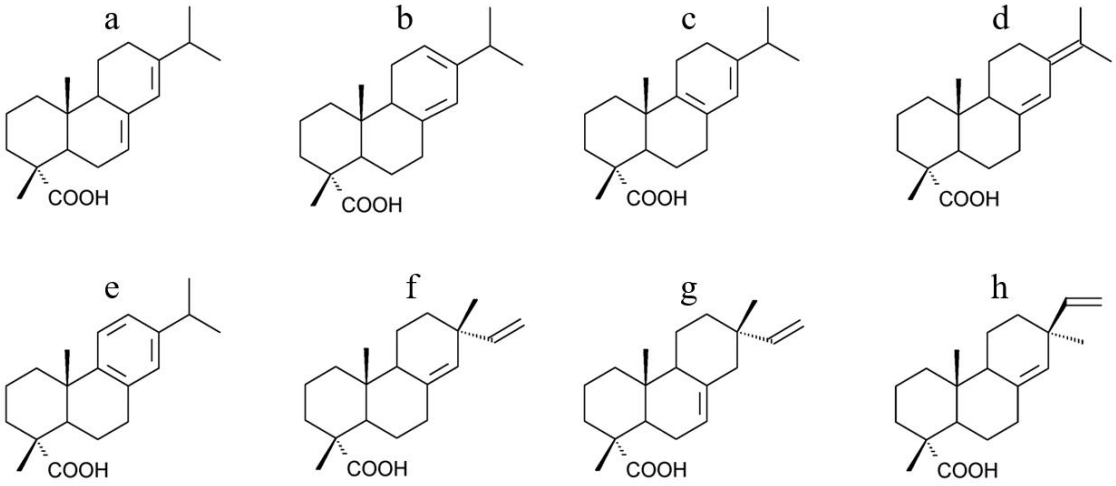

Fig. 1. Chemical structures of resin acids (a) abietic acid, (b) levopimaric acid, (c) palustric acid, (d) neoabietic acid, (e) dehydroabietic acid, (f) sandaracopimaric acid, (g) isopimaric acid, (h) pimaric acid.

MATERIALS AND METHODS

The sequences for the cement protein 20k (CP-20k) *Amphibalanus amphitrite* were retrieved from UniProt (The UniProt Consortium, 2023). Sequences of three CP-20k fragments were obtained for *A. amphitrite* (CP-20k-1, CP-20k-2, CP-20k-3). Accession numbers are K7X3K6, K7XZK5, and K7X9M0, respectively. The 3D structures of *A. amphitrite* fragments were modeled using SWISS-MODEL (Waterhouse et al., 2018). The 3D structures of resin acids (abietic acid, levopimaric acid, palustric acid, neoabietic acid, dehydroabietic acid, sandaracopimaric acid, isopimaric acid and pimaric acid) were retrieved from PubChem (Kim et al., 2023). Molecular docking studies were performed using CB-Dock2 (Liu et al., 2022).

RESULTS

Protein modeling: Because the 3D structures of the three *A. amphitrite* CP-20k fragments were absent in Uniport, 3D structures were obtained using SWISS-MODEL (Waterhouse et al., 2018). When modeling these proteins, templates with the highest coverage and lowest resolution were chosen. As can be seen from Figure 2, each protein fragment has different structures because of its amino acids and molecular interactions.

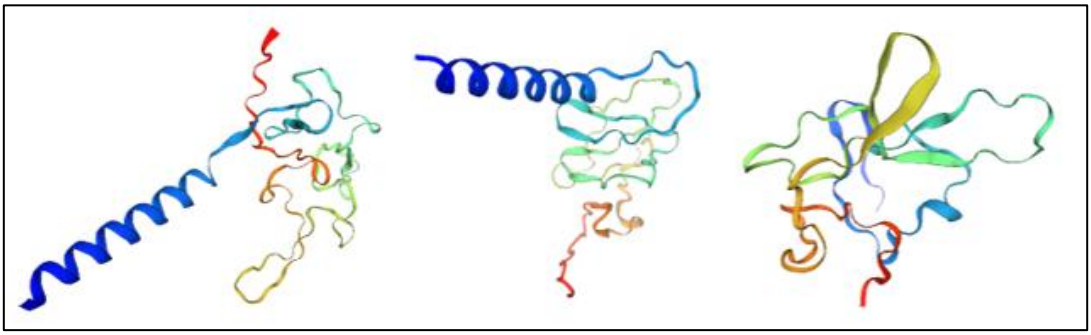

Fig. 2. Modeled 3D structure of *A. amphitrite* CP-20k-1, CP-20k-2, and CP-20k-3 fragments using SWISS-MODEL.

https://doi.org/10.59849/2710-4915.2024.2.13
Available online 31 December 2024

Molecular docking: After modeling all three cement proteins, molecular docking analysis was conducted using CB-Dock2 (Liu et al., 2022). Resin acids were used as ligands. In this section, the molecular docking results of abietic, dehydroabietic, and levopimaric acids, which have the highest binding affinities.

CB-Dock2 predicts the protein-ligand binding sites and calculates the binding effectiveness using a cavity-based detection system. CB-Dock2 predicts five cavities with the lowest binding energies. In Figure 3, instead of giving the results of all binding sites, only cavities with the lowest binding energies are given. Figure 3 shows the molecular interactions between protein fragments and ligands.

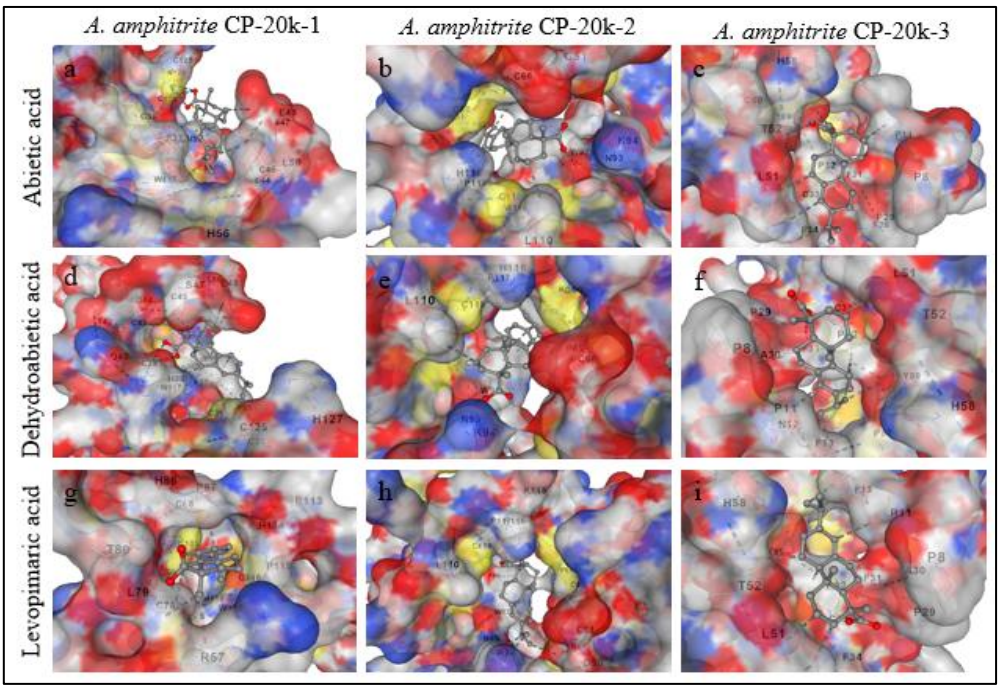

Fig. 3. Molecular docking images of cavities with the highest binding affinities between a) *A. amphitrite* CP-20k-1 and abietic acid, b) *A. amphitrite* CP-20k-2 and abietic acid, c) *A. amphitrite* CP-20k-3 and abietic acid, d) *A. amphitrite* CP-20k-1 and dehydroabietic acid, e) *A. amphitrite* CP-20k-2 and dehydroabietic acid, f) *A. amphitrite* CP-20k-3 and dehydroabietic acid, g) *A. amphitrite* CP-20k-1 and levopimaric acid, h) *A. amphitrite* CP-20k-2 and levopimaric acid, i) *A. amphitrite* CP-20k-3 and levopimaric acid.

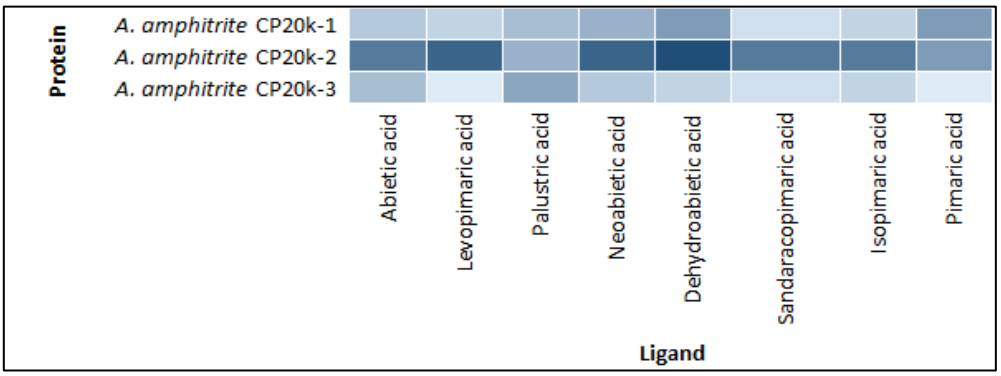

Fig. 4. Molecular docking heatmap of CP20k protein fragments and resin acids (binding affinities are displayed by color. The darker color means lower binding energy, which indicates better binding).

Table 1. Molecular docking results of abietic acid with *Amphibalanus amphitrite* CP-20k-1

Receptor (Protein)	CurPocket ID	Vina Score (kcal/mol	Cavity Volume (Å^3)	Center (x, y, z)	Docking Size (x, y, z)	Contact Residues
Amphibalanus amphitrite CP-20k-1	C1	-6.4	600	2, -1, 1	21, 21, 21	**Chain A**: PRO35 PHE37 CYS39 GLN40 ASP41 THR42 CYS43 ARG57 GLU73 CYS74 ASN75 CYS76 ASN77 LEU79 THR80 SER85 HIS86 PRO87 CYS88 CYS105 ASP106 ILE112 ARG113 HIS114 PRO115 CYS116 TRP117 HIS118 ARG119
	C2	-6.4	357	-8, 0, 11	21, 21, 21	**Chain A**: ALA23 ARG24 GLY25 GLN26 LYS27 ARG28 ASN29 CYS30 ASN31 ASN34 CYS36 ASP106 SER107 ILE108 GLU109 CYS110 SER111 ILE112 ARG113 CYS116 HIS118 GLU120 CYS121 GLY122 CYS123
	C3	-6.9	325	2, 9, 0	21, 21, 21	**Chain A**: CYS30 CYS36 PHE37 HIS38 CYS39 CYS43 ASP44 CYS45 SER47 GLU48 LEU50 HIS56 TRP117 CYS121 GLY122 CYS123 ASN124 CYS125 HIS127
	C4	-5.9	113	-5, 10, 15	21, 21, 21	**Chain A**: CYS30 ASN31 PRO32 ASN34 PRO35 CYS36 PHE37 HIS38 SER47 GLU48 LEU50 CYS123 ASN124 CYS125 THR126 HIS127 THR128 ALA129
	C5	-5.1	36	4, -8, -7	21, 21, 21	**Chain A:** ARG57 HIS60 CYS76 ASN77 HIS78 LEU79 THR80 PRO81 CYS82 ASP83 HIS86 PRO87 CYS88 TRP89 TYR101 ASP102 CYS103 ASP104 CYS105 ASP106 PRO115 TRP117

Table 2. Molecular docking results of abietic acid with *Amphibalanus amphitrite* CP-20k-2

Receptor (Protein)	CurPocket ID	Vina Score (kcal/mol	Cavity Volume (Å^3)	Center (x, y, z)	Docking Size (x, y, z)	Contact Residues
Amphibalanus amphitrite CP-20k-2	C1	-7.6	6765	4, 1, -7	32, 27, 35	**Chain A**: CYS38 GLY39 CYS44 TYR45 TYR46 CYS47 ASP50 CYS51 GLU52 CYS53 HIS54 LEU56 HIS57 ASP58 GLN59 CYS60 LYS61 PRO62 HIS64 PRO65 CYS66 TYR67 ARG68 LEU70 ASP78 CYS79 HIS81 VAL82 LYS83 PRO84 TRP92 ASN93 LYS94 TYR95 THR96 VAL97 GLN103 ASN106 HIS109 LEU110 HIS116 PRO117 CYS118 TRP119
	C2	-6.1	391	-5, -8, -15	21, 21, 21	**Chain A**: CYS85 ASN86 HIS89 CYS91 GLN103 ARG104 CYS105 ASN106 CYS107 ASP108 HIS109 TRP119 HIS120 ARG121 HIS122 CYS123 ASP124 CYS125
	C3	-6.8	89	-8, -11, -7	21, 21, 21	**Chain A**: GLN59 CYS60 LYS61 PRO62 HIS89 CYS112 ASN113 ARG114 LYS115 HIS116 PRO117 CYS118 TRP119 HIS120 CYS123 ASP124 CYS125 TYR126 CYS127 LYS128
	C4	-7.2	72	-1, 4, 10	21, 21, 21	**Chain A**: CYS38 GLY39 PRO40 HIS42 ARG43 CYS44 TYR45 TYR46 CYS47 CYS53 HIS54 LEU56 HIS57 ASP58 GLN59 CYS60 LYS61 SER63 HIS64 PRO65 CYS66 TYR67 PHE75 CYS77 CYS79
	C5	-6.6	42	3, 6, 16	21, 21, 21	**Chain A**: HIS33 LYS34 SER35 ARG36 HIS37 CYS38 GLY39 CYS44 TYR45 TYR46 CYS47 GLU52 CYS53 HIS54 HIS55 LEU56 HIS57 ASP58 GLN59 CYS60 HIS64 CYS66

Table 3. Molecular docking results of abietic acid with *Amphibalanus amphitrite* CP-20k-3

Receptor (Protein)	CurPocket ID	Vina Score (kcal/mol)	Cavity Volume (Å^3)	Center (x, y, z)	Docking Size (x, y, z)	Contact Residues
Amphibalanus amphitrite CP-20k-3	C1	-7.0	3269	1, -3, 1	21, 27, 30	**Chain A**: ASN7 PRO8 PRO11 ASN12 PHE13 ASN14 CYS15 THR16 SER18 CYS19 CYS21 LEU24 PRO28 PRO29 ALA30 PHE31 PRO32 CYS33 PHE34 LEU51 THR52 PRO53 HIS58 CYS60 TRP61 ASP72 ASN73 ASN74 CYS75 ASP76 CYS77 ASP78 ILE80 ALA81 CYS82 SER83 THR84 PRO87 CYS88 TYR89 HIS90 ARG91 GLN92 CYS93 SER94 CYS95 ASP96
	C2	-5.7	110	16, -1, -2	21, 21, 21	**Chain A**: CYS19 ASP20 CYS21 ALA22 GLU23 LEU24 ARG25 ASN40 GLU41 THR42 GLU43 PRO44 SER45 CYS46 ASP47 CYS48 ASN49 HIS90 ARG91 GLN92
	C3	-5.5	107	19, 4, 4	21, 21, 21	**Chain A**: CYS19 ASP20 CYS21 ALA22 GLU23 LEU24 ARG25 CYS27 PRO28 PRO29 CYS33 PHE34 ARG35 LEU36 PRO37 SER38 GLU41 GLU43 PRO44 SER45 CYS46 ASP47 CYS48 ASN49 GLN50 LEU51 TRP61 THR63 LEU70 HIS90 ARG91
	C4	-5.7	89	0, 4, -13	21, 21, 21	**Chain A**: CYS1 LYS2 GLY3 PRO4 PRO5 CYS6 ASN10 PRO11 ASN12 PHE13 ASN14 CYS15 THR16 SER18 CYS19 ASP20 CYS21 GLU23 LEU24 PRO28 PRO29 ALA30 PHE31 PRO32 THR84 SER85 HIS86 PRO87 CYS88
	C5	-6.0	63	16, 6, -4	21, 21, 21	**Chain A**: PRO4 PRO5 CYS6 ASN7 PRO8 ASN12 GLU23 LEU24 ARG25 TYR26 CYS27 PRO28 PRO29 ALA30 PHE31 PRO32 CYS33 PHE34 ARG35 LEU36 PRO37 SER38 GLU41 THR42 GLU43 PRO44 LEU51

Table 4. Molecular docking results of dehydroabietic acid with *Amphibalanus amphitrite* CP-20k-1

Receptor (Protein)	CurPocket ID	Vina Score (kcal/mol)	Cavity Volume (Å^3)	Center (x, y, z)	Docking Size (x, y, z)	Contact Residues
Amphibalanus amphitrite CP-20k-1	C1	-6.7	600	2, -1, 1	20, 20, 20	**Chain A**: PRO35 PHE37 CYS39 GLN40 ASP41 THR42 CYS43 ARG57 CYS58 CYS74 ASN75 CYS76 ASN77 LEU79 THR80 SER85 HIS86 PRO87 CYS88 CYS105 ASP106 ARG113 HIS114 PRO115 CYS116 TRP117 HIS118 ARG119
	C2	-6.0	357	-8, 0, 11	20, 20, 20	**Chain A**: ALA23 ARG24 GLY25 GLN26 LYS27 ARG28 ASN29 ASN31 ASN34 CYS36 ASP106 SER107 ILE108 GLU109 CYS110 SER111 ILE112 ARG113 CYS116 GLU120 CYS121 GLY122 CYS123
	C3	-7.3	325	2, 9, 0	20, 20, 20	**Chain A**: CYS30 PRO35 CYS36 PHE37 HIS38 CYS39 GLN40 THR42 CYS43 ASP44 CYS45 SER46 SER47 GLU48 GLY49 LEU50 PHE51 CYS52 HIS56 VAL72 GLU73 CYS74 TRP117 CYS121 GLY122 CYS123 ASN124 CYS125 HIS127
	C4	-5.7	113	-5, 10, 15	20, 20, 20	**Chain A**: GLN26 LYS27 ARG28 ASN29 CYS30 ASN31 PRO32 ASN34 PRO35 CYS36 PHE37 HIS38 SER47 GLU48 LEU50 CYS123 ASN124 CYS125 THR126 HIS127 THR128 ALA129
	C5	-4.9	36	4, -8, -7	20, 20, 20	**Chain A:** HIS60 GLU73 ASN75 CYS76 ASN77 HIS78 LEU79 THR80 PRO81 CYS82 ASP83 TRP89 TYR101 ASP102 CYS103 ASP104 ASP106 ARG119

Table 5. Molecular docking results of dehydroabietic acid with *Amphibalanus amphitrite* CP-20k-2

Receptor (Protein)	CurPocket ID	Vina Score (kcal/mol)	Cavity Volume (Å^3)	Center (x, y, z)	Docking Size (x, y, z)	Contact Residues
Amphibalanus amphitrite CP-20k-2	C1	-8.0	6765	4, 1, -7	32, 27, 35	**Chain A**: CYS38 CYS44 TYR45 TYR46 CYS47 HIS48 ASP50 CYS51 GLU52 CYS53 HIS54 HIS57 ASP58 CYS60 LYS61 PRO62 HIS64 PRO65 CYS66 TYR67 ARG68 LEU70 ASP78 CYS79 HIS81 VAL82 LYS83 PRO84 CYS85 PRO87 LYS88 HIS89 PRO90 CYS91 TRP92 ASN93 LYS94 TYR95 THR96 VAL97 LYS98 HIS101 LYS102 GLN103 ARG104 CYS105 ASN106 HIS109 LEU110 HIS116 PRO117 CYS118 TRP119
	C2	-6.2	391	-5, -8, -15	20, 20, 20	**Chain A**: CYS85 ASN86 PRO87 HIS89 CYS91 LYS102 GLN103 ARG104 CYS105 ASN106 CYS107 ASP108 HIS109 LEU110 ARG111 CYS112 TRP119 HIS120 ARG121 HIS122 CYS123 ASP124 CYS125
	C3	-6.3	89	-8, -11, -7	20, 20, 20	**Chain A**: CYS60 LYS61 PRO62 LYS88 HIS89 ASP108 LEU110 ARG111 CYS112 ASN113 ARG114 HIS116 PRO117 CYS118 TRP119 HIS120 HIS122 CYS123 ASP124 CYS125 TYR126 CYS127
	C4	-7.3	72	-1, 4, 10	20, 20, 20	**Chain A**: CYS38 GLY39 PRO40 HIS42 ARG43 CYS44 TYR45 TYR46 CYS53 HIS54 HIS55 LEU56 HIS57 ASP58 GLN59 CYS60 LYS61 SER63 HIS64 PRO65 CYS66 TYR67
	C5	-6.5	42	3, 6, 16	20, 20, 20	**Chain A**: HIS33 LYS34 SER35 ARG36 HIS37 CYS38 CYS44 TYR45 TYR46 CYS47 CYS53 HIS54 HIS55 LEU56 HIS57 ASP58 GLN59 HIS64

Table 6. Molecular docking results of dehydroabietic acid with *Amphibalanus amphitrite* CP-20k-3

Receptor (Protein)	CurPocket ID	Vina Score (kcal/mol)	Cavity Volume (Å^3)	Center (x, y, z)	Docking Size (x, y, z)	Contact Residues
Amphibalanus amphitrite CP-20k-3	C1	-6.8	3269	1, -3, 1	26, 27, 30	**Chain A**: ASN7 PRO8 GLY9 ASN10 PRO11 ASN12 PHE13 CYS19 ASP20 CYS21 ALA22 CYS27 PRO28 PRO29 ALA30 PHE31 PRO32 CYS33 PHE34 ARG35 CYS46 ASP47 CYS48 ASN49 LEU51 THR52 SER57 HIS58 THR84 SER85 HIS86 PRO87 CYS88 TYR89 HIS90 ARG91 GLN92
	C2	-5.8	110	16, -1, -2	20, 20, 20	**Chain A**: CYS19 ASP20 CYS21 ALA22 GLU23 LEU24 ARG25 TYR26 CYS33 ARG35 ASN40 GLU41 THR42 GLU43 PRO44 SER45 CYS46 ASP47 CYS48 ASN49 HIS90 ARG91 GLN92
	C3	-5.3	107	19, 4, 4	20, 20, 20	**Chain A**: ASP20 CYS21 ALA22 LEU24 PHE34 ARG35 LEU36 PRO37 SER38 GLY39 ASN40 GLU41 THR42 GLU43 PRO44 SER45 CYS46 ASP47 CYS48 ASN49 GLN50 TRP61 THR63 VAL65 LEU70 ARG91
	C4	-5.8	89	0, 4, -13	20, 20, 20	**Chain A**: CYS1 LYS2 GLY3 PRO4 PRO5 CYS6 ASN10 PRO11 ASN12 PHE13 ASN14 THR16 SER18 ASP20 GLU23 LEU24 PRO28 ALA30 PHE31 THR84 SER85 PRO87
	C5	-5.7	63	16, 6, -4	20, 20, 20	**Chain A**: PRO5 CYS6 ASN12 GLU23 LEU24 ARG25 TYR26 CYS27 PRO28 PRO29 ALA30 PHE31 CYS33 PHE34 ARG35 LEU36 PRO37 SER38 LEU51

Table 7. Molecular docking results of levopimaric acid with *Amphibalanus amphitrite* CP-20k-1

Receptor (Protein)	CurPocket ID	Vina Score (kcal/mol)	Cavity Volume (Å^3)	Center (x, y, z)	Docking Size (x, y, z)	Contact Residues
Amphibalanus amphitrite CP-20k-1	C1	-6.8	600	2, -1, 1	20, 20, 20	**Chain A**: ARG57 CYS58 CYS76 LEU79 THR80 SER85 HIS86 PRO87 CYS88 CYS105 ILE112 ARG113 HIS114 PRO115 CYS116 TRP117 HIS118
	C2	-6.7	357	-8, 0, 11	20, 20, 20	**Chain A**: ALA23 ARG24 GLY25 GLN26 LYS27 ARG28 ASP106 ILE108 GLU109 CYS110 CYS116 HIS118 GLU120 CYS121 CYS123
	C3	-6.3	325	2, 9, 0	20, 20, 20	**Chain A**: CYS36 PHE37 HIS38 CYS39 THR42 CYS43 ASP44 CYS45 SER46 SER47 GLU48 LEU50 PHE51 CYS52 HIS56 VAL72 GLU73 CYS74 TRP117 GLY122 CYS123 ASN124 CYS125 THR126 HIS127
	C4	-5.8	113	-5, 10, 15	20, 20, 20	**Chain A**: ASN29 CYS30 ASN31 PRO32 ASN34 PRO35 CYS36 PHE37 HIS38 GLU48 LEU50 CYS125 THR126 HIS127 THR128 ALA129
	C5	-4.9	36	4, -8, -7	20, 20, 20	**Chain A:** HIS60 ASN75 ASN77 HIS78 LEU79 THR80 PRO81 CYS82 ASP83 TYR101 ASP102 CYS103 ASP104 ASP106

Table 8. Molecular docking results of levopimaric acid with *Amphibalanus amphitrite* CP-20k-2

Receptor (Protein)	CurPocket ID	Vina Score (kcal/mol)	Cavity Volume (Å^3)	Center (x, y, z)	Docking Size (x, y, z)	Contact Residues
Amphibalanus amphitrite CP-20k-2	C1	-7.8	6765	4, 1, -7	32, 27, 35	**Chain A**: ASP50 CYS51 GLU52 CYS60 LYS61 PRO62 HIS64 PRO65 CYS66 TYR67 ARG68 LEU70 PRO71 HIS81 VAL82 LYS83 PRO84 PRO90 TRP92 ASN93 LYS94 TYR95 THR96 VAL97 LYS98 HIS101 LYS102 GLN103 ARG104 CYS105 ASN106 LEU110 LYS115 HIS116 PRO117 CYS118
	C2	-6.1	391	-5, -8, -15	20, 20, 20	**Chain A**: CYS85 ASN86 HIS89 CYS91 LYS102 GLN103 ARG104 CYS105 ASN106 CYS107 ASP108 HIS109 TRP119 HIS120 ARG121 HIS122 CYS123 ASP124
	C3	-6.0	89	-8, -11, -7	20, 20, 20	**Chain A**: GLN59 CYS60 LYS61 PRO62 HIS89 CYS112 ASN113 ARG114 HIS116 PRO117 CYS118 TRP119 HIS120 ARG121 HIS122 CYS123 ASP124 CYS125 TYR126 CYS127
	C4	-7.1	72	-1, 4, 10	20, 20, 20	**Chain A**: CYS38 GLY39 ARG43 CYS44 TYR45 TYR46 CYS47 CYS53 HIS54 HIS55 LEU56 HIS57 ASP58 GLN59 CYS60 LYS61 SER63 HIS64 PRO65 CYS66 TYR67 PHE75 CYS77 CYS79
	C5	-6.2	42	3, 6, 16	20, 20, 20	**Chain A**: HIS33 LYS34 SER35 ARG36 CYS38 GLY39 CYS44 TYR45 TYR46 CYS47 GLU52 CYS53 HIS54 HIS55 LEU56 HIS57 ASP58 GLN59 HIS64

Table 9. Molecular docking results of levopimaric acid with *Amphibalanus amphitrite* CP-20k-3

Receptor (Protein)	CurPocket ID	Vina Score (kcal/mol)	Cavity Volume (Å^3)	Center (x, y, z)	Docking Size (x, y, z)	Contact Residues
Amphibalanus amphitrite CP-20k-3	C1	-6.6	3269	1, -3, 1	26, 27, 30	**Chain A**: ASN7 PRO8 GLY9 PRO11 PHE13 ASN14 THR16 SER18 CYS19 ASP20 CYS21 ALA22 GLU23 LEU24 CYS27 PRO28 PRO29 ALA30 PHE31 PRO32 CYS33 PHE34 ARG35 PRO44 SER45 CYS46 ASP47 CYS48 ASN49 LEU51 THR52 HIS58 TRP61 THR63 LEU70 ASP72 ASN73 ASN74 CYS75 ASP76 CYS77 ASP78 TYR89 HIS90 ARG91 GLN92
	C2	-5.6	110	16, -1, -2	20, 20, 20	**Chain A**: CYS19 ASP20 CYS21 ALA22 GLU23 LEU24 GLU41 THR42 GLU43 PRO44 SER45 CYS46 ASP47 CYS48 ASN49 HIS90 ARG91 GLN92
	C3	-5.5	107	19, 4, 4	20, 20, 20	**Chain A**: ASP20 CYS21 ALA22 LEU24 ARG25 CYS33 LEU36 PRO37 SER38 GLY39 ASN40 GLU41 GLU43 PRO44 SER45 CYS46 ASP47 CYS48 ASN49 TRP61 THR63 LEU70 ARG91
	C4	-5.7	89	0, 4, -13	20, 20, 20	**Chain A**: CYS1 LYS2 GLY3 PRO4 PRO5 CYS6 ASN10 PRO11 ASN12 PHE13 ASN14 CYS15 THR16 SER18 CYS19 ASP20 CYS21 GLU23 LEU24 PRO28 PRO29 ALA30 PHE31 THR84 SER85 PRO87
	C5	-5.6	63	16, 6, -4	20, 20, 20	**Chain A**: PRO4 PRO5 CYS6 GLU23 LEU24 ARG25 TYR26 CYS27 PRO28 PRO29 ALA30 PHE31 CYS33 PHE34 ARG35 PRO37 LEU51

Sometimes cavities with the lowest vina score are not the effective areas for a protein to function. For this reason, the properties of all cavities obtained by CB-Dock2 are presented in Table 1-9. For every interaction, vina scores (kcal/mol), cavity volumes (Å^3) and contact residues are given. Same as before, only the results of abietic, dehydroabietic and levopimaric acids are given. The molecular docking results of the remaining resin acids are given in the Supplementary File (Table S1-S15).

To better visualize the molecular docking results, a heatmap was plotted using Microsoft Excel. As can be seen from Figure 4, the lowest binding energy belongs to dehydroabietic acid and *A. amphitrite* CP20k-2. Moreover, almost all resin acids bind *A. amphitrite* CP20k-2 better than the other two proteins. Generally, binding energies less than -5 kcal/mol indicate better binding affinity (Shuyuan and Haoyu, 2023).

DISCUSSION

Barnacles are a major problem in underwater studies. In the past biocide-containing toxic paints were used to deal with biofouling. After their usage was banned, more and more eco-friendly paints were introduced. However, they are not as effective as toxic paints, and they lose their effectiveness after some time. When paints reach their half-life, hard fouler like barnacles start to accumulate on the surface. Therefore, an investigation must be conducted on how to deal with hard fouling organisms, especially barnacles, in an eco-friendly manner. To do that the attachment mechanisms of barnacles must be enlightened because it is still not clear how they achieve underwater attachment. So far, we know that barnacles use cement to attach to surfaces and this cement contains high amounts of proteins (Walker, 1972; Kamino et al., 1996; Naldrett and Kaplan, 1997; Kamino et al., 2000; Khandeparker and Anil, 2007; Lin et al., 2021). Each protein has different functions in the attachment mechanism. Among them, CP19k and CP20k are thought to be responsible for the attachment (Assadizadeh et al., 2023). Therefore, more studies should be conducted on these proteins. In this paper, the molecular docking of resin acids to the CP20k fragments was studied and promising results were obtained. By looking at our results, one can say that barnacle CP20k fragments and resin acids surely interact with acceptable binding energies. *In silico* studies such as this one may lead to the

development of new compounds with antifouling abilities. New antifouling compounds can be tested using computational analysis methods instead of field tests. In this way, it will be less time and resource-consuming to test the antifouling ability of a compound.

CONCLUSION

A. amphitrite CP20k is a cement protein that barnacles use to attach rigidly to the surfaces. Therefore, studying this cement protein is crucial for understanding its attachment mechanisms. Rosin is a natural compound with antifouling ability. When its composition was studied, it was found that rosin has a high amount of resin acids. These resin acids can be effective molecules in antifouling technologies. Therefore, the interactions between cement protein and resin acids were investigated in this study. Molecular docking results of abietic, dehydroabietic and levopimaric acids are given in the paper. Molecular docking results of the other resin acids are given in the Supplementary File. When all interactions were examined, between the three protein fragments, CP20k-2 had the lowest vina scores, and the best interaction was between *A. amphitrite* CP20k-2 and dehydroabietic acid. These findings are promising in biocide-free antifouling strategies since antifouling properties can be tested before field tests. Biocide-free antifouling coatings will solve the biofouling problem in an eco-friendly way. Thus, it will reduce carbon emissions of ships and biodiversity loss

SUPPORTING MATERIAL

Additional molecular docking results were given.

AUTHOR CONTRIBUTIONS

Ibrahim Kirkiz: Data curation, Investigation, Methodology, Writing - original draft, Writing - review & editing. **Levent Cavas:** Conceptualization, Investigation, Supervision. Writing - review & editing.

COMPETING INTERESTS

The authors declare that they have no known competing financial interests or personal relationships that could have appeared to influence the work reported in this paper.

FUNDING SOURCES

This research did not receive any specific grant from funding agencies in the public, commercial, or not-for-profit sectors.

REFERENCES

Aldred N., Clare A.S. (2008) The adhesive strategies of cyprids and development of barnacle-resistant marine coatings. *Biofouling*, **24(5):** 351-363; doi: 10.1080/08927010802256117.

Almeida J.R., Vasconcelos V. (2015) Natural antifouling compounds: Effectiveness in preventing invertebrate settlement and adhesion. *Biotechnology Advances*, **33(3-4):** 343-357; doi: 10.1016/j.biotechadv.2015.01.013.

Assadizadeh M., Goodarz N., Pak A.H.M., Haghayeghi S.M.H., Irani M.A. (2023) Structural investigation of *Amphibalanus amphitrite* cement proteins: an in silico study. *Bioinspired, Biomimetic and Nanobiomaterials*, **12(4):** 140-152; doi: 10.1680/jbibn.23.00008.

Carve M., Scardino A., Shimeta J. (2019) Effects of surface texture and interrelated properties on marine biofouling: a systematic review. *Biofouling*, **35(6):** 597-617; doi: 10.1080/08927014.2019.1636036.

Cavas L., Dağ C. (2024) In-silico methods in antifouling paint technology. *World Intellectual Property Organization. International Publication Number* WO2024144682A1. https://patents.google.com/patent/WO2024144682A1/en.

Dimkić I., Ristivojević P., Janakiev T., Berić T., Trifković J., Milojković-Opsenica D., Stanković S. (2016) Phenolic profiles and antimicrobial activity of various plant resins as potential botanical sources of Serbian

propolis. *Industrial Crops and Products*, **94:** 856-871; doi: 10.1016/j.indcrop.2016.09.065.

Dreyer N., Zardus J.D., Høeg J.T., Olesen J., Yu M.C., Chan B.K. (2020) How whale and dolphin barnacles attach to their hosts and the paradox of remarkably versatile attachment structures in cypris larvae. *Organisms Diversity & Evolution*, **20:** 233-249; doi: 10.1007/s13127-020-00434-3.

Ewers- Saucedo C., Pappalardo P. (2019) Testing adaptive hypotheses on the evolution of larval life history in acorn and stalked barnacles. *Ecology and Evolution*, **9(19):** 11434-11447; https://doi.org/10.1002/ece3.5645.

Farkas A., Degiuli N., Martić I. (2021) The impact of biofouling on the propeller performance. *Ocean Engineering*, **219:** 108376. https://doi.org/10.1016/j.oceaneng.2020.108376.

Gule N.P., Begum, N.M., Klumperman B. (2016) Advances in biofouling mitigation: A review. *Critical Reviews in Environmental Science and Technology*, **46(6):** 535-555; https://doi.org/10.1080/10643389.2015.1114444

Ip J.C.H., Qiu J.W., Chan B.K. (2021) Genomic insights into the sessile life and biofouling of barnacles (*Crustacea: Cirripedia*). *Heliyon*, **7(6):** e07291; doi: 10.1016/j.heliyon.2021.e07291.

Jonker J.L., Abram F., Pires E., Varela Coelho A., Grunwald I., Power A.M. (2014) Adhesive proteins of stalked and acorn barnacles display homology with low sequence similarities. *PLoS One*, **9(10):** e108902; doi: 10.1371/journal.pone.0108902.

Kamino K. (2013) Mini-review: barnacle adhesives and adhesion. *Biofouling*, **29(6):** 735-749; doi: 10.1080/08927014.2013.800863.

Kamino K. (2016) Barnacle Underwater Attachment. *In: Smith, A. (eds) Biological Adhesives*. Springer: Cham; doi: 10.1007/978-3-319-46082-6_7.

Kamino K., Inoue K., Maruyama T., Takamatsu N., Harayama S., Shizuri Y. (2000) Barnacle cement proteins: importance of disulfide bonds in their insolubility. *Journal of Biological Chemistry*, **275(35):** 27360-27365. https://doi.org/10.1016/S0021-9258(19)61519-X.

Kamino K., Nakano M., Kanai S. (2012) Significance of the conformation of building blocks in curing of barnacle underwater adhesive. *The FEBS Journal*, **279(10):** 1750-1760; doi: 10.1111/j.1742-4658.2012.08552.x.

Kamino K., Odo S., Maruyama,T. (1996) Cement proteins of the acorn-barnacle, Megabalanus rosa. *The Biological Bulletin*, **190(3):** 403-409; doi:10.2307/1543033.

Keeling C.I., Bohlmann J. (2006). Diterpene resin acids in conifers. *Phytochemistry*, **67(22):** 2415-2423; doi: 10.1016/j.phytochem.2006.08.019.

Khandeparker L., Anil A.C. (2007) Underwater adhesion: the barnacle way. *International Journal of Adhesion and Adhesives*, **27(2):** 165-172; doi: 10.1016/j.ijadhadh.2006.03.004.

Kim S., Chen J., Cheng T., Gindulyte A., He J., He S., Li Q., Shoemaker B.A., Thiessen P.A., Yu B., Zaslavsky L., Zhang J., Bolton E.E. (2023). PubChem 2023 update. *Nucleic Acids Research*, **51(D1):** D1373-D1380; doi: 10.1093/nar/gkac956.

Li X., Li S., Huang X., Chen Y., Cheng J., Zhan A. (2021) Protein-mediated bioadhesion in marine organisms: A review. *Marine Environmental Research*, **170:** 105409; doi: 10.1016/j.marenvres.2021.105409.

Liang C., Strickland J., Ye Z., Wu W., Hu B., Rittschof D. (2019) Biochemistry of barnacle adhesion: an updated review. *Frontiers in Marine Science*, **6:** 565; doi: 10.3389/fmars.2019.00565.

Lin H.C., Wong Y.H., Sung C.H., Chan B.K.K. (2021) Histology and transcriptomic analyses of barnacles with different base materials and habitats shed lights on the duplication and chemical diversification of barnacle cement proteins. *BMC Genomics*, **22:** 1-18; https://doi.org/10.1186/s12864-021-08049-4.

Liu J.C.W., Høeg J.T., Chan B.K. (2016) How do coral barnacles start their life in their hosts? *Biology Letters*, **12(6):** 20160124. https://doi.org/10.1098/rsbl.2016.0124.

Liu Y., Yang X., Gan J., Chen S., Xiao Z.X., Cao Y. (2022) CB-Dock2: Improved protein–ligand blind docking by integrating cavity detection, docking and homologous template fitting. *Nucleic Acids Research*, **50(W1):** W159-W164; https://doi.org/10.1093/nar/gkac394.

Martin V.J., Yu Z., Mohn W.W. (1999) Recent

advances in understanding resin acid biodegradation: microbial diversity and metabolism. *Archives of Microbiology*, **172:** 131-138; https://doi.org/10.1007/s002030050752.

Naldrett M.J., Kaplan D.L. (1997) Characterization of barnacle (Balanus eburneus and B. cenatus) adhesive proteins. *Marine Biology*, **127:** 629-635; doi: 10.1007/s002270050053.

Nasrolahi A., Havenhand J., Wrange A.L., Pansch C. (2016) Population and life-stage specific sensitivities to temperature and salinity stress in barnacles. *Scientific Reports*, **6(1):** 32263; https://doi.org/10.1038/srep32263.

Ottavioli J., Paoli M., Casanova J., Tomi F., Bighelli A. (2019) Identification and quantitative determination of resin acids from *Corsican pinus pinaster* Aiton oleoresin using ^{13}C- NMR Spectroscopy. *Chemistry & Biodiversity*, **16(1):** e1800482; doi: 10.1002/cbdv.201800482.

Rocha M., Antas P., Castro L.F.C., Campos A., Vasconcelos V., Pereira F., Cunha I. (2019) Comparative analysis of the adhesive proteins of the adult stalked goose barnacle *Pollicipes pollicipes* (*Cirripedia: Pedunculata*). *Marine Biotechnology*, **21:** 38-51; doi: 10.1007/s10126-018-9856-y.

Sarkar P.K., Pawar S.S., Rath S.K., Kandasubramanian B. (2022) Anti-barnacle biofouling coatings for the protection of marine vessels: synthesis and progress. *Environmental Science and Pollution Research*, **29(18):** 26078-26112; doi: 10.1007/s11356-021-18404-3.

Savluchinske-Feio S., Curto M.J.M., Gigante B., Roseiro J.C. (2006) Antimicrobial activity of resin acid derivatives. *Applied Microbiology and Biotechnology*, **72:** 430-436; doi: 10.1007/s00253-006-0517-0.

Shuyuan L., Haoyu C. (2023) Mechanism of Nardostachyos Radix et Rhizoma–Salidroside in the treatment of premature ventricular beats based on network pharmacology and molecular docking. *Scientific Reports*, **13(1):** 20741; https://doi.org/10.1038/s41598-023-48277-0.

The UniProt Consortium (2023) UniProt: the Universal Protein Knowledgebase in 2023, *Nucleic Acids Research*, **51(D1):** D523-D531; https://doi.org/10.1093/nar/gkac1052.

Walker G. (1972) The biochemical composition of the cement of two barnacle species, Balanus hameri and Balanus crenatus. *Journal of the Marine Biological Association of the United Kingdom*, **52(2):** 429-435; doi: 10.1017/S0025315400018786.

Waterhouse A., Bertoni M., Bienert S., Studer G., Tauriello G., Gumienny R., Heer F., de Beer T.A.P., Rempfer C., Bordoli L., Lepore R., Schwede T. (2018) SWISS-MODEL: homology modelling of protein structures and complexes. *Nucleic Acids Research*, **46(W1):** W296-W303; doi: 10.1093/nar/gky427.

Wong Y.H., Dreyer N., Liu H., Lan Y., Chen J.J., Sun J., ... Chan B.K. (2023) Gene co-option, duplication and divergence of cement proteins underpin the evolution of bioadhesives across barnacle life histories. *Molecular Ecology*, **32(18):** 5071-5088; doi: 10.1111/mec.17084.

Yan G., Sun J., Wang Z., Qian P.Y., He L. (2020) Insights into the synthesis, secretion and curing of barnacle cyprid adhesive via transcriptomic and proteomic analyses of the cement gland. *Marine Drugs*, **18(4):** 186; doi: 10.3390/md18040186.

Yap F.C., Wong W.L., Maule A.G., Brennan G.P., Chong V.C., Lim L.H.S. (2017) First evidence for temporary and permanent adhesive systems in the stalked barnacle cyprid, *Octolasmis angulata*. *Scientific Reports*, **7(1):** 44980; doi: 10.1038/srep44980.

Yebra D.M., Kiil S., Dam-Johansen K. (2004) Antifouling technology - past, present and future steps towards efficient and environmentally friendly antifouling coatings. *Progress in Organic Coatings*, **50(2):** 75-104; https://doi.org/10.1016/j.porgcoat.2003.06.001.

Yuvaraj D., Annushrie A., Niranjana M., Gnanasekaran R., Gopinath M., Iyyappan J. (2021) A review on process and characterization of mussels and cirripeds for adhesive properties and applications thereof. *Current Research in Green and Sustainable Chemistry*, **4:** 100092. https://doi.org/10.1016/j.crgsc.2021.100.

Supplementary Materials

Table S1. Molecular docking results of neoabietic acid with *Amphibalanus amphitrite* CP-20k-1

Receptor (Protein)	CurPocket ID	Vina Score (kcal/mol)	Cavity Volume (Å^3)	Center (x, y, z)	Docking Size (x, y, z)	Contact Residues
Amphibalanus amphitrite CP-20k-1	C1	-7.1	600	2, -1, 1	21, 21, 21	**Chain A**: PRO35 PHE37 CYS39 GLN40 ASP41 THR42 CYS43 ARG57 CYS58 GLU73 CYS74 ASN75 CYS76 ASN77 LEU79 THR80 SER85 HIS86 PRO87 CYS88 ASP104 CYS105 ASP106 ILE112 ARG113 HIS114 PRO115 CYS116 TRP117 HIS118 ARG119
	C2	-6.2	357	-8, 0, 11	21, 21, 21	**Chain A**: ALA23 ARG24 GLY25 GLN26 LYS27 ARG28 CYS36 CYS105 ASP106 SER107 ILE108 GLU109 CYS110 CYS116 HIS118 GLU120 CYS121 GLY122 CYS123 ASN124
	C3	-6.7	325	2, 9, 0	21, 21, 21	**Chain A**: CYS30 CYS36 PHE37 HIS38 CYS39 CYS43 ASP44 CYS45 SER46 SER47 GLU48 LEU50 HIS56 TRP117 GLY122 CYS123 ASN124 CYS125 HIS127
	C4	-6.1	113	-5, 10, 15	21, 21, 21	**Chain A**: CYS30 ASN31 PRO32 ASN34 PRO35 CYS36 PHE37 HIS38 SER47 GLU48 LEU50 CYS123 ASN124 CYS125 THR126 HIS127 THR128 ALA129
	C5	-4.7	36	4, -8, -7	21, 21, 21	**Chain A:** HIS60 ILE61 VAL63 ASN65 ASN77 HIS78 LEU79 THR80 PRO81 CYS82 THR100 TYR101 ASP102 CYS103 ASP104 CYS105 ASP106

Table S2. Molecular docking results of neoabietic acid with *Amphibalanus amphitrite* CP-20k-2

Receptor (Protein)	CurPocket ID	Vina Score (kcal/mol)	Cavity Volume (Å^3)	Center (x, y, z)	Docking Size (x, y, z)	Contact Residues
Amphibalanus amphitrite CP-20k-2	C1	-7.8	6765	4, 1, -7	32, 27, 35	**Chain A**: ASP50 CYS51 GLU52 CYS53 CYS60 LYS61 PRO62 HIS64 PRO65 CYS66 TYR67 ARG68 CYS79 ASN80 VAL82 PRO84 PRO90 TRP92 ASN93 LYS94 TYR95 THR96 VAL97 LYS98 HIS101 LYS102 GLN103 ARG104 CYS105 ASN106 LEU110 LYS115 HIS116 PRO117 CYS118 TRP119
	C2	-6.7	391	-5, -8, -15	21, 21, 21	**Chain A**: CYS85 ASN86 HIS89 CYS91 LYS102 GLN103 ARG104 CYS105 ASN106 CYS107 ASP108 HIS109 LEU110 ARG111 CYS112 TRP119 HIS120 ARG121 HIS122 CYS123 CYS125
	C3	-6.5	89	-8, -11, -7	21, 21, 21	**Chain A**: GLN59 CYS60 LYS61 PRO62 HIS89 CYS107 ASP108 HIS109 LEU110 ARG111 CYS112 ASN113 ARG114 HIS116 PRO117 CYS118 TRP119 HIS120 HIS122 CYS123 ASP124 CYS125 TYR126 CYS127 LYS128
	C4	-7.4	72	-1, 4, 10	21, 21, 21	**Chain A**: HIS33 ARG36 CYS38 GLY39 PRO40 HIS42 ARG43 CYS44 TYR45 TYR46 CYS47 GLU52 CYS53 HIS54 HIS55 LEU56 HIS57 ASP58 GLN59 CYS60 LYS61 HIS64 PRO65 CYS66 TYR67
	C5	-6.8	42	3, 6, 16	21, 21, 21	**Chain A**: HIS33 LYS34 SER35 ARG36 HIS37 CYS38 CYS44 TYR45 TYR46 CYS47 HIS48 GLU52 CYS53 HIS54 HIS55 LEU56 HIS57 ASP58 GLN59 HIS64 CYS66 TYR67

Table S3. Molecular docking results of neoabietic acid with *Amphibalanus amphitrite* CP-20k-3

Receptor (Protein)	CurPocket ID	Vina Score (kcal/mol)	Cavity Volume (Å^3)	Center (x, y, z)	Docking Size (x, y, z)	Contact Residues
Amphibalanus amphitrite CP-20k-3	C1	-6.9	3269	1, -3, 1	21, 27, 30	**Chain A**: ASN7 PRO8 GLY9 PRO11 ASN12 PHE13 ASN14 CYS15 THR16 SER18 CYS19 CYS21 PRO28 PRO29 ALA30 PHE31 PRO32 CYS33 PHE34 LEU51 THR52 SER57 HIS58 ASP78 ILE80 ALA81 CYS82 SER83 PRO87 CYS88 TYR89 HIS90 GLN92 CYS93 SER94 CYS95 ASP96
	C2	-5.4	110	16, -1, -2	21, 21, 21	**Chain A**: CYS19 ASP20 CYS21 ALA22 GLU23 LEU24 ARG25 GLU41 THR42 GLU43 PRO44 SER45 CYS46 ASP47 CYS48 ASN49 TYR89 HIS90 ARG91 GLN92
	C3	-5.8	107	19, 4, 4	21, 21, 21	**Chain A**: ASP20 CYS21 ALA22 LEU24 CYS33 LEU36 PRO37 SER38 GLY39 ASN40 GLU41 GLU43 PRO44 SER45 CYS46 ASP47 CYS48 ASN49 GLN50 TRP61 THR63 VAL65 LEU70 HIS90 ARG91
	C4	-6.0	89	0, 4, -13	21, 21, 21	**Chain A**: CYS1 GLY3 PRO4 PRO5 CYS6 ASN7 ASN10 PRO11 ASN12 PHE13 ASN14 CYS15 THR16 SER18 CYS19 ASP20 CYS21 GLU23 LEU24 PRO28 ALA30 PHE31 PRO32 THR84 SER85 PRO87 CYS88 TYR89
	C5	-5.7	63	16, 6, -4	21, 21, 21	**Chain A**: PRO4 PRO5 CYS6 ASN7 ASN12 GLU23 LEU24 ARG25 TYR26 CYS27 PRO28 PRO29 ALA30 PHE31 CYS33 PHE34 ARG35 LEU36 PRO37 LEU51

Table S4. Molecular docking results of palustiric acid with *Amphibalanus amphitrite* CP-20k-1

Receptor (Protein)	CurPocket ID	Vina Score (kcal/mol)	Cavity Volume (Å^3)	Center (x, y, z)	Docking Size (x, y, z)	Contact Residues
Amphibalanus amphitrite CP-20k-1	C1	-6.4	600	2, -1, 1	21, 21, 21	**Chain A**: PRO35 PHE37 CYS39 GLN40 ASP41 THR42 CYS43 ARG57 GLU73 CYS74 ASN75 CYS76 ASN77 LEU79 THR80 SER85 HIS86 PRO87 CYS88 CYS105 ASP106 ILE112 ARG113 HIS114 PRO115 CYS116 TRP117 HIS118 ARG119
	C2	-7.0	357	-8, 0, 11	21, 21, 21	**Chain A**: ALA23 ARG24 GLY25 GLN26 LYS27 ARG28 ASP106 SER107 ILE108 GLU109 CYS110 SER111 CYS116 GLU120 CYS121 GLY122 CYS123
	C3	-6.8	325	2, 9, 0	21, 21, 21	**Chain A**: CYS30 PRO35 CYS36 PHE37 HIS38 CYS39 GLN40 CYS43 ASP44 CYS45 SER47 GLU48 LEU50 HIS56 TRP117 CYS121 GLY122 CYS123 ASN124 CYS125 THR126 HIS127
	C4	-5.8	113	-5, 10, 15	21, 21, 21	**Chain A**: ASN29 CYS30 ASN31 PRO32 ASN34 PRO35 CYS36 PHE37 HIS38 CYS39 SER47 GLU48 LEU50 GLY122 CYS123 ASN124 CYS125 THR126 HIS127 THR128
	C5	-5.1	36	4, -8, -7	21, 21, 21	**Chain A:** HIS60 GLU73 ASN75 CYS76 ASN77 HIS78 LEU79 THR80 PRO81 CYS82 TRP89 TYR101 ASP102 CYS103 ASP104 CYS105 ASP106 ARG119

Table S5. Molecular docking results of palustiric acid with *Amphibalanus amphitrite* CP-20k-2

Receptor (Protein)	CurPocket ID	Vina Score (kcal/mol)	Cavity Volume ($Å^3$)	Center (x, y, z)	Docking Size (x, y, z)	Contact Residues
Amphibalanus amphitrite CP-20k-2	C1	-7.9	6765	4, 1, -7	32, 27, 35	**Chain A**: CYS38 CYS44 TYR45 TYR46 ASP50 CYS51 GLU52 CYS53 HIS54 HIS55 LEU56 HIS57 ASP58 GLN59 CYS60 LYS61 PRO62 HIS64 PRO65 CYS66 TYR67 ARG68 LEU70 ASP78 HIS81 VAL82 LYS83 PRO84 CYS85 CYS91 TRP92 ASN93 LYS94 TYR95 THR96 VAL97 LYS98 HIS101 LYS102 GLN103 ARG104 CYS105 ASN106 HIS109 LEU110 HIS116 PRO117 CYS118 TRP119
	C2	-6.3	391	-5, -8, -15	21, 21, 21	**Chain A**: CYS85 ASN86 HIS89 CYS91 GLN103 ARG104 CYS105 ASN106 CYS107 ASP108 HIS109 LEU110 ARG111 CYS112 PRO117 CYS118 TRP119 HIS120 ARG121 HIS122 CYS123 ASP124 CYS125
	C3	-7.0	89	-8, -11, -7	21, 21, 21	**Chain A**: GLN59 CYS60 LYS61 PRO62 HIS89 ASP108 LEU110 ARG111 CYS112 ASN113 ARG114 LYS115 HIS116 PRO117 CYS118 TRP119 HIS120 HIS122 CYS123 ASP124 CYS125 TYR126 CYS127 LYS128
	C4	-7.1	72	-1, 4, 10	21, 21, 21	**Chain A**: CYS38 GLY39 PRO40 HIS42 ARG43 CYS44 TYR45 TYR46 CYS47 CYS53 HIS54 LEU56 HIS57 ASP58 GLN59 CYS60 LYS61 SER63 HIS64 PRO65 CYS66 TYR67
	C5	-6.6	42	3, 6, 16	21, 21, 21	**Chain A**: HIS33 LYS34 SER35 ARG36 CYS38 ARG43 CYS44 TYR45 TYR46 CYS47 HIS48 GLU52 CYS53 HIS54 HIS55 LEU56 HIS57 ASP58 GLN59 HIS64 CYS66

Table S6. Molecular docking results of palustiric acid with *Amphibalanus amphitrite* CP-20k-3

Receptor (Protein)	CurPocket ID	Vina Score (kcal/mol)	Cavity Volume ($Å^3$)	Center (x, y, z)	Docking Size (x, y, z)	Contact Residues
Amphibalanus amphitrite CP-20k-3	C1	-7.2	3269	1, -3, 1	21, 27, 30	**Chain A**: PRO4 CYS6 ASN7 PRO8 GLY9 ASN10 PRO11 ASN12 PHE13 ASN14 CYS15 THR16 SER18 CYS19 ASP20 CYS21 GLU23 LEU24 TYR26 PRO28 PRO29 ALA30 PHE31 PRO32 CYS33 PHE34 LEU51 THR52 SER57 HIS58 CYS60 TRP61 ASP72 ASN73 ASN74 CYS75 ASP76 CYS77 ASP78 ILE80 ALA81 CYS82 SER83 PRO87 CYS88 TYR89 HIS90 ARG91 GLN92 CYS93 SER94 CYS95 ASP96
	C2	-6.0	110	16, -1, -2	21, 21, 21	**Chain A**: CYS19 ASP20 CYS21 ALA22 GLU23 LEU24 ARG25 TYR26 PRO28 ASN40 GLU41 THR42 GLU43 PRO44 SER45 CYS46 ASP47 CYS48 ASN49 HIS90 ARG91 GLN92
	C3	-5.5	107	19, 4, 4	21, 21, 21	**Chain A**: CYS19 ASP20 CYS21 ALA22 LEU24 ARG25 PHE34 LEU36 PRO37 SER38 GLY39 ASN40 GLU41 GLU43 PRO44 SER45 CYS46 ASP47 CYS48 ASN49 GLN50 TRP61 THR63 VAL65 LEU70 HIS90 ARG91
	C4	-6.2	89	0, 4, -13	21, 21, 21	**Chain A**: CYS1 LYS2 GLY3 PRO4 PRO5 CYS6 GLY9 ASN10 PRO11 ASN12 PHE13 ASN14 THR16 SER18 CYS19 ASP20 CYS21 GLU23 LEU24 PRO28 ALA30 PHE31 THR84 SER85 CYS88
	C5	-6.0	63	16, 6, -4	21, 21, 21	**Chain A**: PRO4 PRO5 CYS6 ASN7 ASN12 GLU23 LEU24 ARG25 TYR26 CYS27 PRO28 PRO29 ALA30 PHE31 PRO32 CYS33 PHE34 ARG35 LEU36 PRO37 SER38 LEU51

Table S7. Molecular docking results of sandaracopimaric acid with *Amphibalanus amphitrite* CP-20k-1

Receptor (Protein)	CurPocket ID	Vina Score (kcal/mol)	Cavity Volume (Å^3)	Center (x, y, z)	Docking Size (x, y, z)	Contact Residues
Amphibalanus amphitrite CP-20k-1	C1	-6.6	600	2, -1, 1	20, 20, 20	**Chain A**: ARG57 CYS76 LEU79 THR80 SER85 HIS86 PRO87 CYS88 CYS105 ILE112 ARG113 HIS114 PRO115 CYS116 TRP117 HIS118
	C2	-6.2	357	-8, 0, 11	20, 20, 20	**Chain A**: ALA23 ARG24 GLY25 GLN26 LYS27 ARG28 ASN29 ASN31 ASN34 CYS36 ASP106 SER107 ILE108 GLU109 CYS110 SER111 ILE112 ARG113 CYS116 HIS118 GLU120 CYS121 GLY122 CYS123
	C3	-6.7	325	2, 9, 0	20, 20, 20	**Chain A**: CYS36 PHE37 HIS38 CYS39 THR42 CYS43 ASP44 CYS45 SER46 SER47 GLU48 GLY49 LEU50 PHE51 CYS52 HIS56 TRP117 CYS123 CYS125 HIS127
	C4	-5.6	113	-5, 10, 15	20, 20, 20	**Chain A**: GLN26 LYS27 ARG28 ASN29 CYS30 ASN31 PRO32 ASN34 PRO35 CYS36 PHE37 HIS38 SER47 GLU48 LEU50 CYS123 CYS125 THR126 HIS127 THR128 ALA129
	C5	-4.8	36	4, -8, -7	20, 20, 20	**Chain A:** HIS60 ILE61 HIS62 VAL63 ASN77 HIS78 LEU79 THR80 PRO81 CYS82 ASP83 HIS86 TRP89 TYR101 ASP102 CYS103 ASP104 ASP106

Table S8. Molecular docking results of sandaracopimaric acid with *Amphibalanus amphitrite* CP-20k-2

Receptor (Protein)	CurPocket ID	Vina Score (kcal/mol)	Cavity Volume (Å^3)	Center (x, y, z)	Docking Size (x, y, z)	Contact Residues
Amphibalanus amphitrite CP-20k-2	C1	-7.6	6765	4, 1, -7	32, 27, 35	**Chain A**: CYS38 CYS44 TYR45 TYR46 CYS47 ASP50 CYS51 GLU52 CYS53 HIS54 LEU56 HIS57 ASP58 GLN59 CYS60 LYS61 HIS64 PRO65 CYS66 TYR67 ARG68 LEU70 HIS81 VAL82 LYS83 PRO84 CYS85 CYS91 TRP92 ASN93 LYS94 TYR95 THR96 VAL97 GLN103 LEU110 LYS115 HIS116 PRO117 CYS118
	C2	-6.1	391	-5, -8, -15	20, 20, 20	**Chain A**: CYS85 ASN86 HIS89 CYS91 LYS102 GLN103 ARG104 CYS105 ASN106 CYS107 ASP108 HIS109 LEU110 ARG111 CYS112 TRP119 HIS120 ARG121 HIS122 CYS123 ASP124 CYS125
	C3	-6.3	89	-8, -11, -7	20, 20, 20	**Chain A**: GLN59 CYS60 LYS61 PRO62 HIS89 CYS112 ASN113 ARG114 LYS115 HIS116 PRO117 CYS118 TRP119 HIS120 CYS123 ASP124 CYS125 TYR126 CYS127
	C4	-7.1	72	-1, 4, 10	20, 20, 20	**Chain A**: CYS38 GLY39 PRO40 HIS42 ARG43 CYS44 TYR45 TYR46 CYS47 GLU52 CYS53 HIS54 LEU56 HIS57 ASP58 GLN59 CYS60 LYS61 HIS64 PRO65 CYS66 TYR67
	C5	-6.5	42	3, 6, 16	20, 20, 20	**Chain A**: GLY32 HIS33 LYS34 SER35 ARG36 CYS38 GLY39 CYS44 TYR45 TYR46 CYS47 HIS48 GLU52 CYS53 HIS54 HIS55 LEU56 HIS57 ASP58 GLN59 HIS64

Table S9. Molecular docking results of sandaracopimaric acid with *Amphibalanus amphitrite* CP-20k-3

Receptor (Protein)	CurPocket ID	Vina Score (kcal/mol)	Cavity Volume (Å^3)	Center (x, y, z)	Docking Size (x, y, z)	Contact Residues
Amphibalanus amphitrite CP-20k-3	C1	-6.7	3269	1, -3, 1	26, 27, 30	**Chain A**: CYS6 ASN7 PRO8 PRO11 ASN12 PHE13 ASN14 THR16 CYS19 ASP20 CYS21 ALA22 LEU24 PRO28 PRO29 ALA30 PHE31 PRO32 CYS33 PHE34 LEU36 SER45 CYS46 ASP47 CYS48 ASN49 LEU51 THR52 SER57 HIS58 CYS60 TRP61 THR63 ASP72 ASN73 ASN74 CYS75 ASP76 CYS77 ASP78 THR84 SER85 HIS86 PRO87 TYR89 HIS90 ARG91 GLN92 CYS93
	C2	-5.5	110	16, -1, -2	20, 20, 20	**Chain A**: CYS19 ASP20 CYS21 ALA22 GLU23 LEU24 ARG25 CYS33 GLU41 THR42 GLU43 PRO44 SER45 CYS46 ASP47 CYS48 ASN49 HIS90 ARG91 GLN92
	C3	-5.5	107	19, 4, 4	20, 20, 20	**Chain A**: ASP20 CYS21 ALA22 GLU23 LEU24 ARG25 PHE34 ARG35 LEU36 PRO37 SER38 GLY39 ASN40 GLU41 THR42 GLU43 PRO44 SER45 CYS46 ASP47 CYS48 ASN49 GLN50 TRP61 THR63 VAL65 LEU70 ARG91
	C4	-5.4	89	0, 4, -13	20, 20, 20	**Chain A**: CYS1 LYS2 GLY3 PRO4 PRO5 CYS6 ASN10 PRO11 ASN12 PHE13 ASN14 THR16 SER18 LEU24 PRO28 PRO29 ALA30 PHE31 THR84 SER85
	C5	-5.8	63	16, 6, -4	20, 20, 20	**Chain A**: GLY3 PRO4 PRO5 CYS6 ASN7 ASN12 GLU23 LEU24 ARG25 TYR26 CYS27 PRO28 PRO29 ALA30 PHE31 PRO32 CYS33 PHE34 ARG35 LEU36 PRO37 SER38 LEU51

Table S10. Molecular docking results of isopimaric acid with *Amphibalanus amphitrite* CP-20k-1

Receptor (Protein)	CurPocket ID	Vina Score (kcal/mol)	Cavity Volume (Å^3)	Center (x, y, z)	Docking Size (x, y, z)	Contact Residues
Amphibalanus amphitrite CP-20k-1	C1	-6.1	600	2, -1, 1	20, 20, 20	**Chain A**: CYS39 ASP41 THR42 CYS43 ARG57 CYS58 GLU73 CYS74 ASN75 CYS76 ASN77 LEU79 THR80 SER85 HIS86 PRO87 CYS88 CYS105 ASP106 ILE112 ARG113 HIS114 PRO115 CYS116 TRP117 HIS118 ARG119
	C2	-6.2	357	-8, 0, 11	20, 20, 20	**Chain A**: ALA23 ARG24 GLY25 GLN26 LYS27 ARG28 ASN29 ASN31 ASN34 CYS36 ASP106 SER107 ILE108 GLU109 CYS110 SER111 ILE112 ARG113 CYS116 HIS118 GLU120 CYS121 GLY122 CYS123
	C3	-6.8	325	2, 9, 0	20, 20, 20	**Chain A**: CYS30 PRO35 CYS36 PHE37 HIS38 CYS39 THR42 CYS43 ASP44 CYS45 SER46 SER47 GLU48 GLY49 LEU50 PHE51 CYS52 HIS56 VAL72 GLU73 CYS74 TRP117 GLY122 CYS123 ASN124 CYS125 HIS127
	C4	-5.7	113	-5, 10, 15	20, 20, 20	**Chain A**: CYS30 ASN31 PRO32 ASN34 PRO35 CYS36 PHE37 HIS38 SER47 GLU48 LEU50 GLY122 CYS123 ASN124 CYS125 THR126 HIS127 THR128 ALA129
	C5	-5.0	36	4, -8, -7	20, 20, 20	**Chain A:** HIS60 ILE61 HIS62 VAL63 SER64 GLU73 ASN75 ASN77 HIS78 LEU79 THR80 PRO81 CYS82 ASP102 CYS103 ASP104 CYS105 ASP106

Table S11. Molecular docking results of isopimaric acid with *Amphibalanus amphitrite* CP-20k-2

Receptor (Protein)	CurPocket ID	Vina Score (kcal/mol)	Cavity Volume (Å^3)	Center (x, y, z)	Docking Size (x, y, z)	Contact Residues
Amphibalanus amphitrite CP-20k-2	C1	-7.6	6765	4, 1, -7	32, 27, 35	**Chain A**: TYR49 ASP50 CYS51 GLU52 CYS60 LYS61 PRO62 PRO65 CYS66 TYR67 ARG68 LYS69 LEU70 PRO71 GLY72 SER73 ASP78 HIS81 VAL82 LYS83 CYS85 PRO90 TRP92 ASN93 LYS94 TYR95 THR96 VAL97 LYS98 HIS101 LYS102 GLN103 ARG104 ASN106 CYS107 HIS109 LEU110 LYS115 HIS116 PRO117 CYS118 TRP119
	C2	-6.2	391	-5, -8, -15	20, 20, 20	**Chain A**: CYS85 ASN86 HIS89 CYS91 LYS102 GLN103 ARG104 CYS105 ASN106 CYS107 ASP108 HIS109 LEU110 ARG111 CYS112 TRP119 HIS120 ARG121 HIS122 CYS123 CYS125
	C3	-6.5	89	-8, -11, -7	20, 20, 20	**Chain A**: GLN59 CYS60 LYS61 PRO62 CYS112 ASN113 ARG114 LYS115 HIS116 PRO117 CYS118 TRP119 HIS120 CYS123 ASP124 CYS125 TYR126 CYS127 LYS128 HIS129
	C4	-7.0	72	-1, 4, 10	20, 20, 20	**Chain A**: CYS38 GLY39 PRO40 HIS42 ARG43 CYS44 TYR45 TYR46 CYS47 CYS53 HIS54 HIS55 LEU56 HIS57 ASP58 GLN59 CYS60 LYS61 SER63 HIS64 PRO65 CYS66 TYR67
	C5	-6.8	42	3, 6, 16	20, 20, 20	**Chain A**: HIS33 LYS34 SER35 ARG36 HIS37 CYS38 HIS42 ARG43 CYS44 TYR45 TYR46 CYS47 CYS53 HIS54 HIS55 LEU56 HIS57 ASP58 HIS64a

Table S12. Molecular docking results of isopimaric acid with *Amphibalanus amphitrite* CP-20k-3

Receptor (Protein)	CurPocket ID	Vina Score (kcal/mol)	Cavity Volume (Å^3)	Center (x, y, z)	Docking Size (x, y, z)	Contact Residues
Amphibalanus amphitrite CP-20k-3	C1	-6.8	3269	1, -3, 1	26, 27, 30	**Chain A**: ASN7 PRO8 ASN10 PRO11 ASN12 PHE13 CYS21 CYS27 PRO28 PRO29 ALA30 PHE31 PRO32 CYS33 PHE34 ARG35 CYS46 ASP47 CYS48 ASN49 LEU51 THR52 PRO53 ASP55 SER57 HIS58 TRP61 THR63 LEU70 ASP72 ASN73 ASN74 CYS75 ASP76 CYS77 ASP78 THR84 SER85 HIS86 PRO87 TYR89 HIS90 ARG91
	C2	-5.6	110	16, -1, -2	20, 20, 20	**Chain A**: CYS19 ASP20 CYS21 ALA22 GLU23 LEU24 ARG25 ASN40 GLU41 THR42 GLU43 PRO44 SER45 CYS46 ASP47 CYS48 ASN49 HIS90 ARG91 GLN92
	C3	-5.5	107	19, 4, 4	20, 20, 20	**Chain A**: CYS21 ALA22 LEU24 CYS27 PRO28 PRO29 PHE31 CYS33 PHE34 ARG35 LEU36 PRO37 SER38 ASN40 GLU41 THR42 GLU43 PRO44 SER45 CYS46 ASP47 CYS48 ASN49 TRP61 THR63 LEU70 ARG91
	C4	-5.6	89	0, 4, -13	20, 20, 20	**Chain A**: CYS1 LYS2 GLY3 PRO4 PRO5 CYS6 ASN10 PRO11 ASN12 PHE13 ASN14 THR16 SER18 ASP20 LEU24 PRO28 ALA30 PHE31 THR84 SER85
	C5	-5.5	63	16, 6, -4	20, 20, 20	**Chain A**: PRO4 PRO5 CYS6 ASN12 GLU23 LEU24 ARG25 TYR26 CYS27 PRO28 PRO29 ALA30 PHE31 PRO32 CYS33 PHE34 ARG35 LEU36 PRO37 SER38 LEU51

Table S13. Molecular docking results of pimaric acid with *Amphibalanus amphitrite* CP-20k-1

Receptor (Protein)	CurPocket ID	Vina Score (kcal/mol)	Cavity Volume (Å^3)	Center (x, y, z)	Docking Size (x, y, z)	Contact Residues
Amphibalanus amphitrite CP-20k-1	C1	-6.8	600	2, -1, 1	20, 20, 20	**Chain A**: ARG57 CYS58 CYS76 LEU79 THR80 SER85 HIS86 PRO87 CYS88 CYS105 ILE112 ARG113 HIS114 PRO115 CYS116 TRP117 HIS118
	C2	-6.2	357	-8, 0, 11	20, 20, 20	**Chain A**: ALA23 ARG24 GLY25 GLN26 LYS27 ARG28 CYS36 CYS105 ASP106 SER107 ILE108 GLU109 CYS110 SER111 CYS116 HIS118 GLU120 CYS121 GLY122 CYS123
	C3	-7.3	325	2, 9, 0	20, 20, 20	**Chain A**: CYS30 PRO35 CYS36 PHE37 HIS38 CYS39 GLN40 THR42 CYS43 ASP44 CYS45 SER46 SER47 GLU48 LEU50 HIS56 TRP117 CYS123 ASN124 CYS125 THR126 HIS127
	C4	-5.6	113	-5, 10, 15	20, 20, 20	**Chain A**: ASN29 CYS30 ASN31 PRO32 ASN34 PRO35 CYS36 PHE37 HIS38 SER47 GLU48 LEU50 GLY122 CYS123 CYS125 THR126 HIS127 THR128 ALA129
	C5	-4.9	36	4, -8, -7	20, 20, 20	**Chain A:** HIS60 ILE61 HIS62 VAL63 ASN77 HIS78 LEU79 THR80 PRO81 CYS82 ASP83 TYR101 ASP102 CYS103

Table S14. Molecular docking results of pimaric acid with *Amphibalanus amphitrite* CP-20k-2

Receptor (Protein)	CurPocket ID	Vina Score (kcal/mol)	Cavity Volume (Å^3)	Center (x, y, z)	Docking Size (x, y, z)	Contact Residues
Amphibalanus amphitrite CP-20k-2	C1	-7.3	6765	4, 1, -7	32, 27, 35	**Chain A**: CYS38 CYS44 TYR45 TYR46 CYS47 CYS51 CYS53 HIS54 HIS55 LEU56 HIS57 ASP58 GLN59 CYS60 LYS61 HIS64 PRO65 CYS66 TYR67 ARG68 VAL82 TRP92 ASN93 LYS94 TYR95 THR96 VAL97 LYS98 HIS101 LYS102 GLN103 ARG104 CYS105 ASN106 LEU110 LYS115 HIS116 PRO117 CYS118
	C2	-6.1	391	-5, -8, -15	20, 20, 20	**Chain A**: CYS85 ASN86 HIS89 PRO90 CYS91 LYS102 GLN103 ARG104 CYS105 ASN106 CYS107 ASP108 HIS109 LEU110 ARG111 CYS112 TRP119 HIS120 ARG121 HIS122 CYS123 ASP124 CYS125
	C3	-6.0	89	-8, -11, -7	20, 20, 20	**Chain A**: GLN59 PRO62 CYS112 ASN113 ARG114 LYS115 HIS116 PRO117 CYS118 TRP119 HIS120 CYS123 ASP124 CYS125 TYR126 CYS127
	C4	-7.0	72	-1, 4, 10	20, 20, 20	**Chain A**: CYS38 GLY39 PRO40 HIS42 ARG43 CYS44 TYR45 TYR46 CYS47 CYS53 HIS54 HIS55 LEU56 HIS57 ASP58 GLN59 CYS60 LYS61 HIS64 PRO65 CYS66 TYR67
	C5	-6.2	42	3, 6, 16	20, 20, 20	**Chain A**: GLU25 GLY32 HIS33 LYS34 SER35 ARG36 HIS37 CYS38 GLY39 HIS42 CYS44 TYR45 TYR46 CYS47 GLU52 CYS53 HIS54 HIS55 LEU56 HIS57 ASP58

Table S15. Molecular docking results of pimaric acid with *Amphibalanus amphitrite* CP-20k-3

Receptor (Protein)	CurPocket ID	Vina Score (kcal/mol)	Cavity Volume (Å^3)	Center (x, y, z)	Docking Size (x, y, z)	Contact Residues
Amphibalanus amphitrite CP-20k-3	C1	-6.6	3269	1, -3, 1	26, 27, 30	**Chain A**: ASN7 PRO8 PRO11 ASN12 PHE13 ASN14 CYS15 THR16 SER18 ASP20 CYS21 GLU23 LEU24 PRO28 PRO29 ALA30 PHE31 PRO32 CYS33 PHE34 LEU51 THR52 HIS58 CYS60 TYR89
	C2	-5.3	110	16, -1, -2	20, 20, 20	**Chain A**: CYS19 ASP20 CYS21 ALA22 GLU23 LEU24 ARG25 LEU36 ASN40 GLU41 THR42 GLU43 PRO44 SER45 CYS46 ASP47 CYS48 ASN49 HIS90 ARG91 GLN92
	C3	-5.2	107	19, 4, 4	20, 20, 20	**Chain A**: ASP20 CYS21 ALA22 LEU24 PHE34 ARG35 LEU36 PRO37 SER38 GLY39 ASN40 GLU41 THR42 GLU43 PRO44 SER45 CYS46 ASP47 CYS48 ASN49 GLN50 TRP61 THR63 VAL65 LEU70 ARG91
	C4	-5.5	89	0, 4, -13	20, 20, 20	**Chain A**: CYS1 LYS2 GLY3 PRO4 PRO5 CYS6 ASN10 PRO11 ASN12 PHE13 ASN14 THR16 LEU24 PRO28 ALA30 PHE31 THR84 SER85
	C5	-5.4	63	16, 6, -4	20, 20, 20	**Chain A**: PRO4 PRO5 CYS6 ASN7 ASN12 GLU23 LEU24 ARG25 TYR26 CYS27 PRO28 PRO29 ALA30 PHE31 CYS33 PHE34 ARG35 LEU36 PRO37 LEU51

ORCID:
Levent Cavas: https://orcid.org/0000-0003-2136-6928
Ibrahim Kirkiz: https://orcid.org/0000-0002-1602-1901